Arch. Metall. Mater. **63** (2018), 4, 1785-1792

DOI: 10.24425/amm.2018.125105

P. KAWULOK*#, I. SCHINDLER*, R. KAWULOK*, P. OPĚLA*, R. SEDLÁČEK**

INFLUENCE OF HEATING PARAMETERS ON FLOW STRESS CURVES OF LOW-ALLOY Mn-Ti-B STEEL

Influence of the initial grain size on hot deformation behavior of the low-alloy Mn-Ti-B steel was investigated. The uniaxial compression tests were performed in range of the deformation temperatures of 900-1200°C and strain rates of 0.1-10 s^{-1}. One set of samples was heated directly to the deformation temperature, which corresponded to the initial austenitic grain size of 19-56 μm; the other set of samples was uniformly preheated at the temperature of 1200°C. Whereas the values of activation energy, peak stress and steady-state stress values practically did not depend on the initial austenitic grain size, the peak strain values of coarser-grained structure significantly increase mainly at high values of the Zener-Hollomon parameter. This confirms the negative effect of the large size of the initial grain on the dynamic recrystallization kinetics, which can be explained by the reduction in nucleation density.

Keywords: Initial austenition grain size, peak stress, peak strain, Mn-Ti-B steel

1. Introduction

An important variable in the material forming process is flow stress or true stress σ (MPa) depending on true (logarithmic) strain ε (-). The true stress – true strain curves are given mainly by material characteristics (chemical composition, phase composition), deformation temperature T (°C), strain rate $\dot{\varepsilon}$ (s^{-1}) and ongoing hardening and dynamic softening processes. The shape of the true stress – true strain curves is basically affected by the type of softening – recovery or recrystallization in progress. From an experimental point of view, it is easiest to obtain data for the prediction of both coordinates of peak point from the set of true stress – true strain curves affected by dynamic recrystallization (DRX). The vertical coordinate of the peak σ_p (MPa) corresponds to the maximum flow stress (peak stress) of the material at the given temperature and strain rate, its horizontal coordinate ε_p (-) approximately corresponds to the critical strain ε_c (-) required for invoking of DRX under the given conditions. We mostly assume the following relation $\varepsilon_c = (0.60 \div 0.83) \cdot \varepsilon_p$ [1, 2]. Values of ε_p and σ_p depend on the Zener-Hollomon parameter Z (s^{-1}), representing the temperature-compensated strain rate [3]:

$$Z = \dot{\varepsilon} \cdot \exp\left(\frac{Q}{R \cdot T}\right) \tag{1}$$

where Q ($J \cdot mol^{-1}$) is the apparent activation energy of hot deformation (the experimental activation energy associated with the temperature dependence of the flow stress [4], the activation energy for dominant diffusion [5]), T (K) is the deformation temperature, and $R = 8.314\ J \cdot mol^{-1} \cdot K^{-1}$ is the universal gas constant.

From the methodological and practical point of view, there is an interesting influence of the initial grain size D_0 (μm) on the development of the flow stress curves. When σ_p and ε_p of the explored material are described mathematically for a uniform D_0 value, it is the most scientific, because it precisely defines the experimental conditions. The application of these relations in practice is, however, limited, because the grain is gradually refined by recrystallization during multi-pass hot forming. For example, in hot-strip mills or bar mills, very fine grain sizes can be produced between passes and this effect influences the subsequent deformation and recrystallization behavior [6]. Therefore, it would be more practicable to predict the coordinates of the peak point with the initial grain size decreasing with the forming temperature decreasing.

The main objective of the works performed with the low-alloy Mn-Ti-B steel was to experimentally verify how the true stress – true strain curves and material constants used for describing the σ_p and ε_p values are affected by two different methods of material heating before deformation – with uniform high-temperature preheating (ensuring an identical initial coarse-grain structure), or with heating directly to the forming temperature (with the D_0 value corresponding to the changing heating temperature).

Dynamic recrystallization is an important mechanism for the microstructure evolution control which frequently takes place under hot forming of materials with low to medium stacking fault energy [4,7]. The experimental DRX study is facilitated by

* VSB-TECHNICAL UNIVERSITY OF OSTRAVA, FACULTY OF METALLURGY AND MATERIALS ENGINEERING, 17. LISTOPADU 15/2172, 708 33 OSTRAVA-PORUBA, CZECH REPUBLIC
** OSTROJ A.S., TĚŠÍNSKÁ 1586/66, 74641 OPAVA, CZECH REPUBLIC
# Corresponding author: petr.kawulok@vsb.cz

information obtained not only from metallography, but also from analyzing the true stress – true strain curves. Practical use of this softening mechanism is, however, limited by the need to invoke a relatively large critical strain which significantly increases in the given material with decreasing temperature and increasing strain rate – the empiric commonly applicated relation is [8]:

$$\varepsilon_p = U \cdot Z^W \tag{2}$$

where U and W are material constants.

The study of DRX in relation to the grain size is complicated by many factors. These are mainly various DRX types or mechanisms. These have a major impact on the shape of the stress-strain curve [7,9-11]. Conventional DRX usually occurs through a discontinuous mechanism, involving nucleation and growth of strain-free grains, i.e. by serration, bulging, and then migration of original high-angle grain boundaries [6,12]. Dynamic recovery as well as twinning can significantly affect the DRX kinetics and shape of stress-strain curves, especially for larger initial grain sizes [13-15].

A higher D_0 value is usually associated with increasing flow stress [6,16,17], whereas in the case of specific stresses σ_p or σ_{ss} (MPa) (related to the steady-state area), the knowledge of various authors is not clearly identical [13,16,18]. Initial fine-grain structure is considered as a factor that significantly accelerates the development of DRX, because the pre-existing grain boundary fraction determines the nucleation density [2,6,13,14]. The reduction of available nucleation sites by decreasing the grain boundary area per unit volume is responsible for the observed change in the dynamic recrystallization behavior. Due to the lack of grain boundaries in coarser grained structures (e.g. materials in the cast state) the intragranular nucleation process becomes predominant. Therefore, structural heterogeneities such as deformation bands, twins and high angle grain boundaries forming during plastic deformation serve as nucleation sites [2,6,19].

2. Experimental procedure

When studying the effect of the initial grain size on the deformation behavior and development of DRX, the custom is to pre-arrange structures with different D_0 value – for instance, by material extrusion at different temperatures [17] and different extrusion ratios [20], or by various procedures of annealing of formed material (see, for instance, [2,16,19]).

In the case of a low-alloy Mn-Ti-B steel, a different approach was applied. The deformation behavior of samples uniformly preheated to the temperature of 1200°C and samples heated directly to the deformation temperature (900-1000-1100-1200°C) was compared. The chemical composition of steel supplied in the form of a hot-formed bar was as follows: 0.28 C-1.20 Mn-0.22 Si-0.028 Ti-0.0031 B (in wt%). Cylindrical samples with a diameter of 10 mm and height of 15 mm were made from the supplied material. These were subjected to a uniaxial compression with a height reduction corresponding to the true strain of 1.0 on the Hydrawedge II module of the Gleeble 3800 hot deformation simulator. Two regimes of thermomechanical sample processing were chosen:

- heating at the rate of $5°C \cdot s^{-1}$ directly to the deformation temperature and forming after holding at this temperature lasting for 120 s; under this regime, four additional samples were quenched in water after heating to a different temperature and the fixed structure was then subjected to metallographic analysis;
- heating at the rate of $5°C \cdot s^{-1}$ to the uniform temperature of 1200°C, holding 120 s, decreasing by rate of $5°C \cdot s^{-1}$ to the deformation temperature, holding 30 s and forming.

The computer-registered dataset was used to draw the true stress – true strain curves and the real mean strain rate was determined for each test, ranging close to the nominal strain rate (0.1-1-10 s^{-1}). Subsequent processing of the results used these values of mean strain rate. The coordinates of the peak point (i.e. ε_p and σ_p) were determined for each true stress – true strain curve. These coordinates were then described in dependence on the temperature, strain rate and in a simplified way also on initial grain size D_0.

The chosen temperature interval falls within existence of austenite, which was also confirmed by the dilatometric test (temperature Ac_3 = 810°C). Fig. 1 shows the etched boundaries

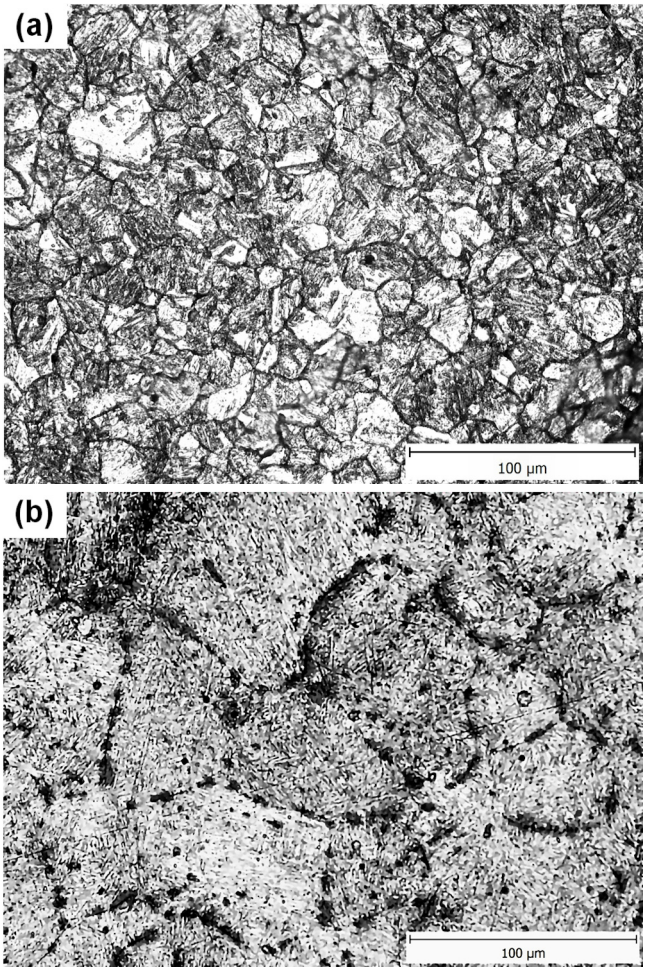

Fig. 1. Metallographic images of the selected samples after etching of the boundaries of the original austenitic grains: (a) temperature of 900°C, D_0 = 19 µm; (b) temperature of 1200°C, D_0 = 56 µm

of the original austenitic grains following heating temperatures of 1200°C and 900°C. The diagram in Fig. 2 indicates that value D_0 was increasing depending on the temperature almost in a linear manner under the given conditions.

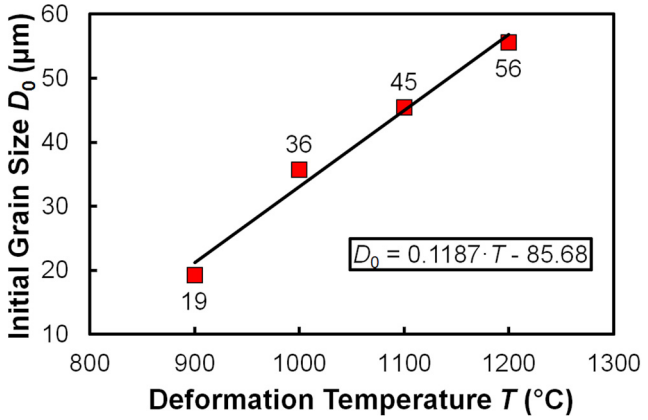

Fig. 2. Influence of deformation temperature on the initial size of austenitic grains

3. Mathematical processing of experimental data

The diagrams in Fig. 3 indicate the effect of T, $\dot{\varepsilon}$ and D_0 on flow stress and the coordinates of peak point.

The constants in the equation describing the relation between σ_p, T and $\dot{\varepsilon}$ were first determined separately for two sets of data (with/without preheating at 1200°C). The hyperbolic law in the Arrhenius type equation is conventionally used for its determination [21]:

$$\dot{\varepsilon} = C \cdot \exp\left(\frac{-Q}{R \cdot T}\right) \cdot \left[\sinh\left(\alpha \cdot \sigma_p\right)\right]^n \tag{3}$$

where, besides the activation energy Q (J·mol^{-1}), C (s^{-1}), n (-) and α (MPa^{-1}) are material constants. This relationship is often solved by a simple graphic method, based on the repeatedly used linear regression. A particularity of the sinh function is used in this calculation that enables simplifying the Eq. (3) for low stress values into the form of the Arrhenius power law:

$$\dot{\varepsilon} = C_1 \cdot \exp\left(\frac{-Q}{R \cdot T}\right) \cdot \sigma_p{}^n \tag{4}$$

and, vice versa, for high stress values into the form of exponential law:

$$\dot{\varepsilon} = C_2 \cdot \exp\left(\frac{-Q}{R \cdot T}\right) \cdot \exp\left(\beta \cdot \sigma_p\right) \tag{5}$$

where C_1 (s^{-1}), C_2 (s^{-1}) and β (MPa^{-1}) are the material constants. The constant a in Eq. (3) is given by the relationship of $\alpha = \beta/n$. For a chosen high-temperature level (i.e. for low stress values)

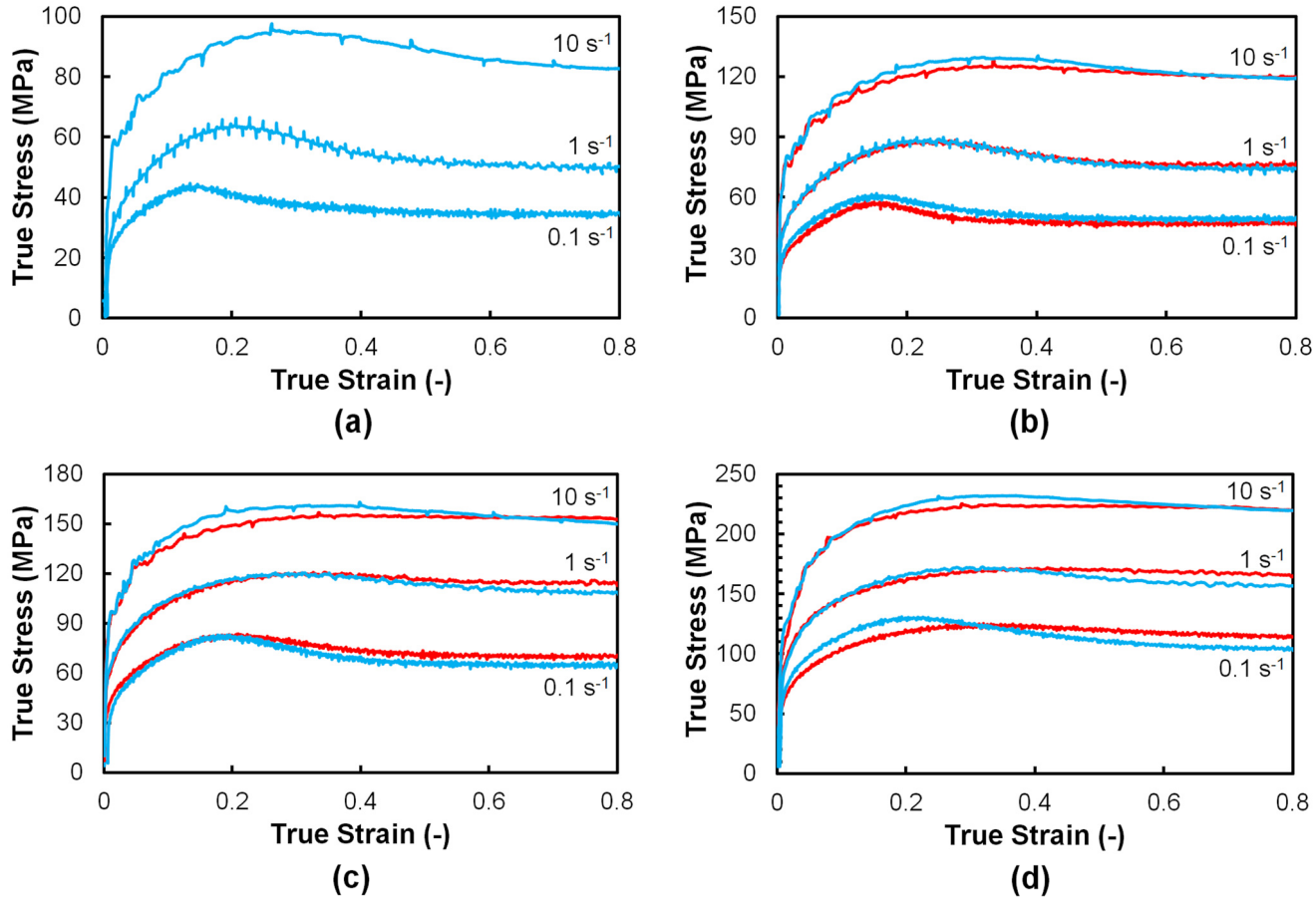

Fig. 3. Comparison of the true stress – true strain curves (blue lines – direct heating to forming temperature; red lines –preheating at 1200°C; the $\dot{\varepsilon}$ – values are nominal): (a) temperature of 1200°C; (b) temperature of 1100°C; (c) temperature of 1000°C; (d) temperature of 900°C

the constant n is determined by the linear regression of the experimentally found σ_p – values in coordinates $\ln \dot{\varepsilon} \sim \ln \sigma_p$, and for a chosen low-temperature level (i.e. for high stress values) the constant β is obtained by the linear regression in coordinates $\ln \dot{\varepsilon} \sim \sigma_p$. After the calculation of the value α, the constants Q and C in Eq. (3) may be obtained by the final linear regression of all the data plotted in the coordinate system $\ln \dot{\varepsilon} - n \cdot \ln [\sinh (\alpha \cdot \sigma_p)] \sim T^{-1}$. The diagrams in Fig. 4 document this simplified procedure, whereas regressions were calculated only for cases of direct heating to the deformation temperature (blue squares) and red triangles corresponding to preheating at 1200°C were added to the diagrams only for purposes of comparison.

Such an estimate of constants n and β is a weak point of the described method, since it can be strongly influenced by the selection of the corresponding temperature level and by the experimental data scatter. This deficiency has been eliminated by application of the specially developed software ENERGY 4.0 [22], which enables an interactive elimination of points showing the excessive deviation from the trends specified in a graphic way. The software uses the values of n and β, determined by the above-mentioned procedure, only as the first estimate of parameters for the final refining by nonlinear regression of all the data corresponding to the Eq. (3). Such regression for ensuring higher precision of results (i.e. constants Q, C, n and α) is very unstable without the preliminary estimation of the chosen material constants.

Final Q values calculated for both sets of tests were then used to describe strain ε_p by power function – see Fig. 5.

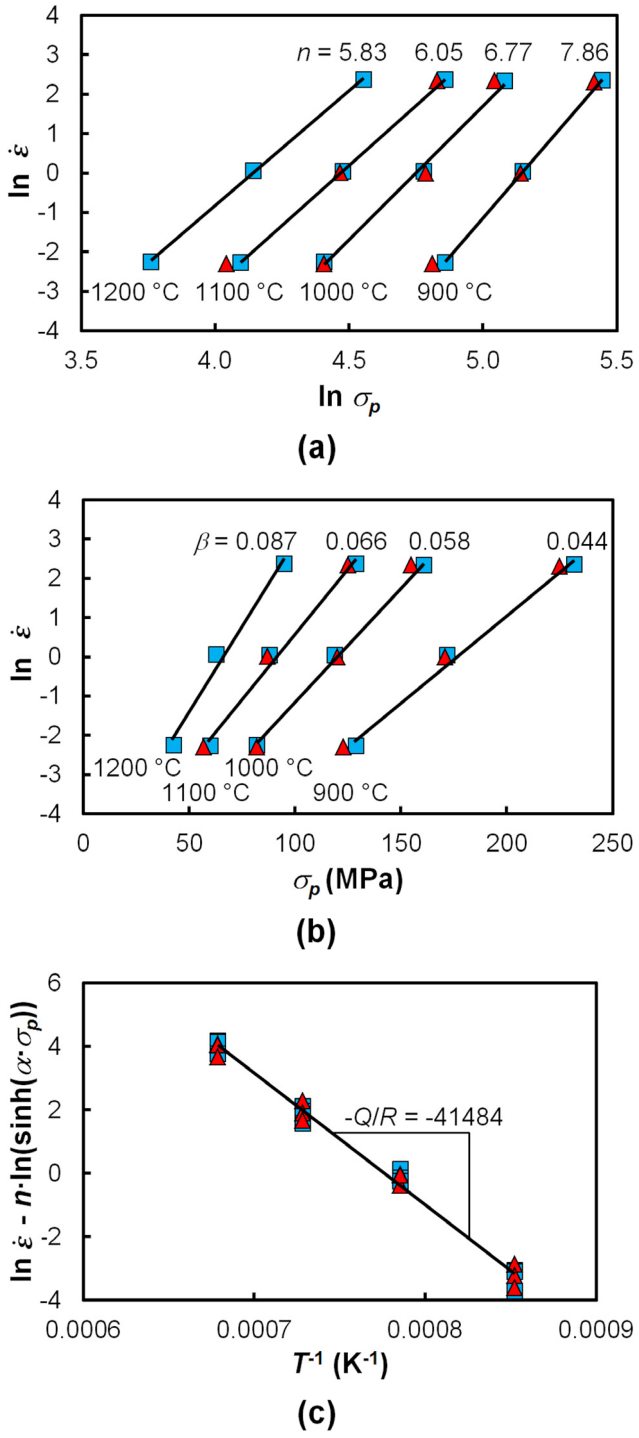

Fig. 4. Calculation of constants in Eq. (3) for conditions of direct heating to the deformation temperature: (a) calculation of $n = 5.83$; (b) calculation of $\beta = 0.044$; (c) calculation of $Q = 345$ kJ·mol^{-1}

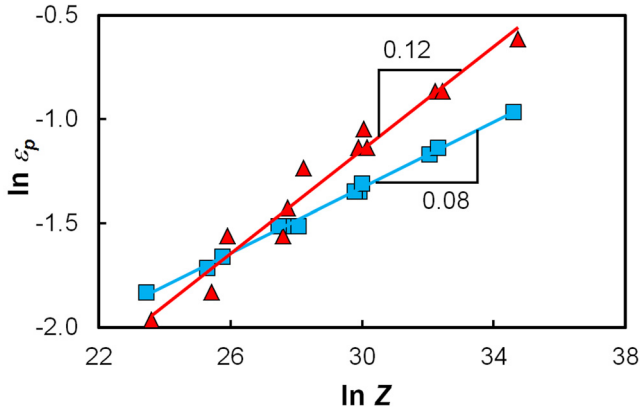

Fig. 5. Determination of W constants in Eq. (2) for the cases of heating of samples directly to the deformation temperature (blue squares), or after preheating at a temperature of 1200°C (red triangles)

Table 1 summarizes all constants calculated by the above-mentioned procedures. Calculation Mode 1 corresponds to a simple procedure with repeated use of linear regression (see Fig. 4), Mode 2 is based on specifying non-linear regression; that resulted in a decrease in value of Q of about 10 % as compared to the simple calculation.

TABLE 1

Constants in equations describing the coordinates of peak point of low-alloy Mn-Ti-B steel

Materials constants	Mode of heating		
	Direct to deformation temperatures		Preheating
	Calc. Mode 1	Calc. Mode 2	Calc. Mode 2
Q (kJ·mol^{-1})	345.1	314.5	316.5
n (-) (1200°C)	5.83	5.90	5.94
α (MPa) (900°C)	0.0076	0.0054	0.0058
C (s^{-1})	$9.8 \cdot 10^{13}$	$6.7 \cdot 10^{13}$	$6.0 \cdot 10^{13}$
U (-)	0.022	0.023	0.008
W (-)	0.08	0.08	0.12

4. Discussion of results

The shape of the flow stress curves of low-alloy Mn-Ti-B steel in Fig. 3 indicates that with decreasing temperature and increasing strain rate, the peak stresses monotonously move towards larger strain and stress. The influence of initial coarser grain (D_0 = 56 μm vs 45 μm) is almost imperceptible at the deformation temperature of 1100°C, small at the temperature of 1000°C (D_0 = 56 μm vs 36 μm) and evident at the temperature of 900°C (D_0 = 56 μm vs 19 μm). Coarser grain with the size of 56 μm, obtained by preheating at the temperature of 1200°C, retards DRX initiation and increases strain ε_p. It makes the flow stress curves flatter, which, however, influences the stress values σ_p or σ_{ss} only slightly. This knowledge notably corresponds to, e.g. results of Ohadi, Parsa and Mirzadeh [13] achieved with AISI 304L stainless steel.

The findings of Mirzadeh, Parsa and Ohadi [23] about the flow stress curves of AISI 304L steel affected by the initial grain size in combination with temperature and strain rate are more complicated. For the cases shown in Fig. 6, some differences in the shape of the flow stress curves are evident. Whereas coarser grain results in higher flow stress at deformation temperature of 1100°C and strain rate of 0.01 s^{-1}, it significantly reduces flow stress at temperature of 900°C and strain rate of 0.01 s^{-1} or 0.1 s^{-1}. By increasing the initial grain size, the range of flow stress becomes tighter (see 900°C – 0.1 s^{-1} flow stress curves) and the characteristic DRX peak tends to vanish (see 900°C – 0.01 s^{-1} flow stress curves). The DRX peaks in the samples with fine-grained microstructure are more apparent than the other ones, which can be related to the feasibility of DRX to occur in the material with small grain size due to the increase in the density of nucleation sites.

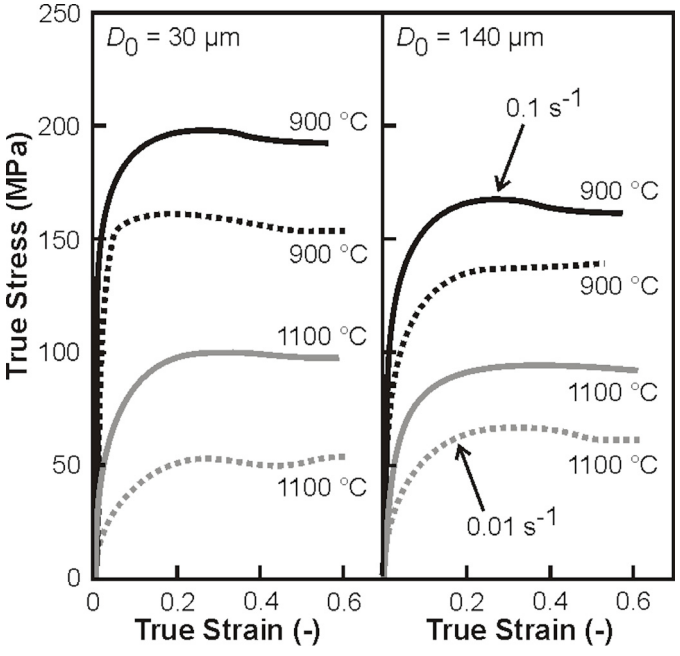

Fig. 6. Influence of initial size (D_0 = 30-140 μm) on flow stress curves of 304L steel at the temperature of 900-1100°C and strain rate of 0.01-0.1 s^{-1} – according to [23]

Comparison of the constants in Table 1 (particularly for more precise Calculation Mode 2) indicates that preheating at 1200°C became significantly evident in the case of the description of strain ε_p by Eq. (2), whereas constants Q, n, α and C related to stress σ_p change only slightly – compare, for instance, the values of activation energy 314.5 kJ · mol^{-1} (in the case of heating directly to the deformation temperature) against 316.5 kJ · mol^{-1} (following grain coarsening by preheating at the temperature of 1200°C). However, it should be pointed out that constants in TABLE 1 corresponding to direct heating to changing forming temperature only have a phenomenological character, because they do not reflect the fully identical initial condition of material (at least, as for the initial austenitic grain size, changing within the range of 19-56 μm).

For similar steels, we can find very close values of activation energy during hot forming in the literature. Sellars and Tegart [24] state the value of Q = 304 kJ · mol^{-1} for steel with 0.25% C. Equation derived by Medina and Hernandez [25] reflects the content of C, Mn, Si, Mo, Ti, V and Nb to a limited extent. It results in Q = 295.2 kJ · mol^{-1} for the tested low-alloy Mn-Ti-B steel. A simpler relation of Colàs [26] only works with the content of C, Mn and Si, however, giving result almost identical to the experimentally determined value for low-alloy Mn-Ti-B steel – Q = 316.7 kJ · mol^{-1}. Unlike the relation stated in [25], the Q value increases with the increasing content of carbon in this equation, which appeared to be more realistic.

Applying the constants obtained, we can calculate stress $\sigma_p = f(Z)$ using the equation derived from Eq. (3):

$$\sigma_p = \frac{1}{\alpha} \cdot \arcsin h \sqrt[n]{\frac{Z}{C}} = \frac{1}{\alpha} \cdot \left\{ \left(\frac{Z}{C}\right)^{1/n} + \left[\left(\frac{Z}{C}\right)^{2/n} + 1 \right]^{1/2} \right\} \quad (6)$$

This relation is very useful, because it enables fast prediction of the maximum flow stress of the given material at the specific values of temperature and strain rate. Relations of the Eq. (3) and Eq. (6) type including calculation of Q-value on the basis thereof, find their physical justification in calculations applying stress σ_p and σ_{ss}. Very often it is the expansion of Eq. (6) into the form of a constitutive equation, reflecting the effect of strain and enabling the description of flow stress curves with function $\sigma = f(Z, \varepsilon)$. This is resolved by strain compensation of the constitutive equation or, as the case may be, by determining the regressive relations of Q, n, α and C on the strain size. The fifth order polynomials were applied the most often to represent the influence of strain on these parameters – see, for instance, prediction of flow stress for 42CrMo steel [27], Ti-6Al-4V titanium alloy [28] or Al-Cu-Li aluminium alloy [29]. Other researchers applied the fourth order polynomials in this case, e.g. to describe the flow stress curves of 15Cr-15Ni-2.2Mo Ti-modified stainless steel [30] or AZ61 magnesium alloy [31]. On the other hand, Mohamadizadeh, Zarei-Hanzaki and Abedi [32] described the deformation behavior of 0.8C-17Mn-8Al low-density steel applying a more complex approach and described the relations $\alpha = f(\varepsilon, T)$, $n = f(\varepsilon, T)$, $Q = f(\varepsilon, \dot{\varepsilon}, T)$ and $C = f(\varepsilon, \dot{\varepsilon}, T)$.

The accuracy of the mathematical description of both coordinates of peak point in dependence on the Zener-Hollomon parameter is given in Table 2 and Table 3, whereas it can also be evaluated by the diagrams shown in Fig. 7. The derived relations using the constants in Table 1 (applying the Calculation Mode 2) describe the given parameters in a very reliable manner, however, there is evident a bigger scatter of the experimental values ε_p (see also Fig. 5).

TABLE 2

Accuracy of the description of peak stress σ_p and peak strain ε_p in the case of heating directly to the deformation temperature

T	$\dot{\varepsilon}$	σ_p (MPa)		Error	ε_p (-)		Error
(°C)	(s^{-1})	Measured	Calculated	(%)	Measured	Calculated	(%)
1200	0.106	43	44	2.3	0.14	0.16	14.3
1200	1.07	63	64	1.6	0.21	0.19	–9.5
1200	10.8	95	93	–2.1	0.29	0.23	–20.7
1100	0.104	60	60	0.0	0.15	0.18	20.0
1100	1.05	88	87	–1.1	0.23	0.22	–4.3
1100	10.7	129	124	–3.9	0.33	0.26	–21.2
1000	0.105	82	85	3.7	0.20	0.22	10.0
1000	1.05	119	121	1.7	0.29	0.26	–10.3
1000	10.3	161	167	3.7	0.34	0.32	–5.9
900	0.104	129	125	–3.1	0.22	0.27	22.7
900	1.05	172	173	0.6	0.29	0.32	10.3
900	10.5	232	230	–0.9	0.34	0.39	14.7
Mean error (%)				0.2			1.7
Standard deviation (%)				2.4			14.8

TABLE 3

Accuracy of description of peak stress σ_p and peak strain ε_p in the case of preheating to the temperature of 1200°C

T	$\dot{\varepsilon}$	σ_p (MPa)		Error	ε_p (-)		Error
(°C)	(s^{-1})	Measured	Calculated	(%)	Measured	Calculated	(%)
1200	0.106	43	44	2.3	0.14	0.14	0.0
1200	1.07	63	64	1.6	0.21	0.19	–9.5
1200	10.8	95	92	–3.2	0.29	0.25	–13.8
1100	0.100	57	59	3.5	0.16	0.18	12.5
1100	1.01	87	85	–2.3	0.24	0.23	–4.2
1100	10.4	125	121	–3.2	0.35	0.31	–11.4
1000	0.100	82	84	2.4	0.21	0.23	9.5
1000	1.00	120	119	–0.8	0.32	0.31	–3.1
1000	10.3	155	164	5.8	0.42	0.41	–2.4
900	0.100	123	123	0.0	0.32	0.32	0.0
900	1.00	171	169	–1.2	0.42	0.42	0.0
900	10.0	225	223	–0.9	0.54	0.56	3.7
Mean error (%)				0.3			–1.6
Standard deviation (%)				2.7			7.5

The diagrams in Fig. 4 and Fig. 7 suggest that values σ_p are affected by the applied sample heating methods only slightly. This is even more evident from the comparative diagram shown in Fig. 8. Using derived equations, the calculated, i.e. predicted values $\sigma_p = f(Z)$ almost do not depend on the initial grain size;

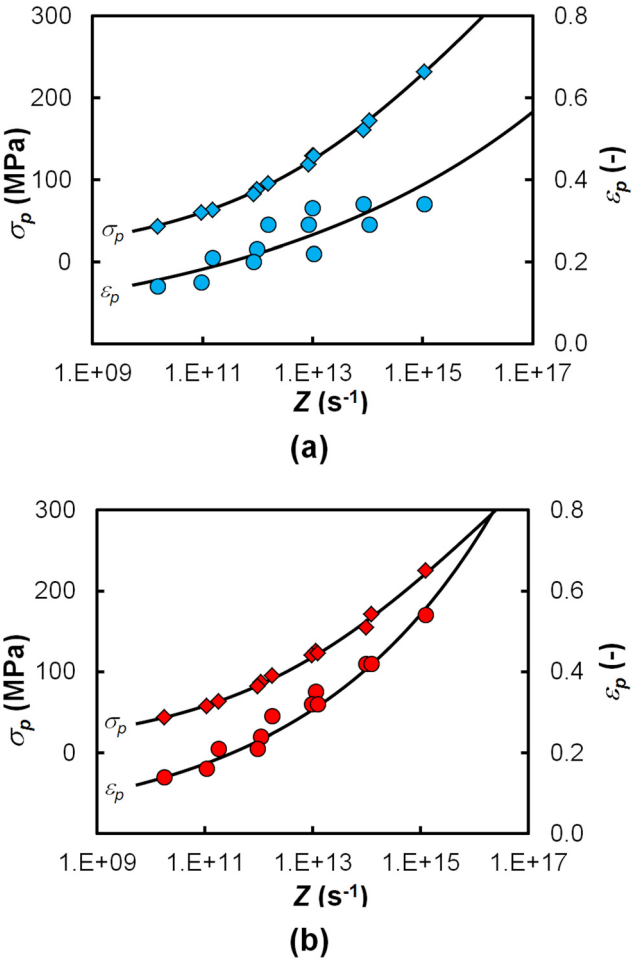

Fig. 7. Comparison of experimental values of ε_p and σ_p (points) with predicted values (lines): (a) heating directly to the deformation temperature; (b) preheating at the temperature of 1200°C

we can only observe a minor decrease in the peak stress values in coarser-grained structure at high values of parameter Z. The situation is quite different in the case of relation $\varepsilon_p = f(Z)$ – coarser-grained structure is much more difficult to recrystallize, which results in higher strain ε_p mainly at high strain rates and low deformation temperatures. At the lowest values of parameter Z,

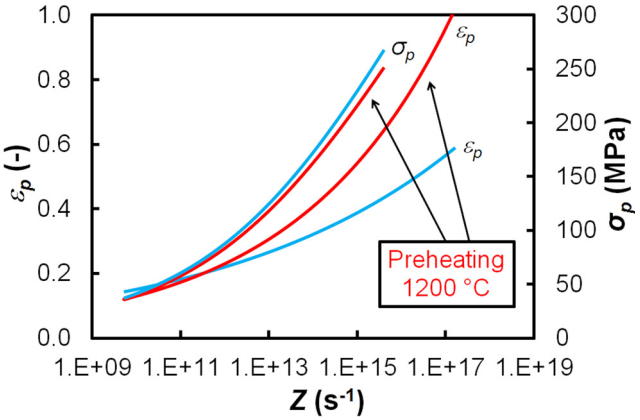

Fig. 8. Effect of the Zener-Hollomon parameter on predicted values of σ_p and ε_p (blue lines – heating directly to the deformation temperature; red lines – preheating at high temperatures; values ε_p were extrapolated for the values of parameter Z outside the experimental range)

two ε_p values were found to be slightly higher in finer-grained structure than in coarser-grained structure (see also Fig. 5), but this is probably the consequence of the scatter of experimental data or, as the case may be, accuracy of localization of peak stresses in flat flow stress curves.

Medina and Hernandez [33] gathered a huge quantity of data from literature and their own data of material constants B, $p1$ and $p2$ in this equation:

$$\varepsilon_p = B \cdot D_0^{p1} \cdot Z^{p2} \tag{7}$$

The experiment carried out with low-alloy Mn-Ti-B steel qualitatively confirmed the effect of both the initial grain size and temperature-compensated strain rate on peak strain, but regressive determination of the constants B, $p1$ and $p2$ is complicated by different Q values for both sets of tests. The equation obtain, therefore, has a somewhat indicative character:

$$\varepsilon_p = 0.024 \cdot D_0^{0.38} \cdot Z^{0.11} \tag{8}$$

As evident from Fig. 9, the accuracy of the strain $\varepsilon_p = f(D_0,Z)$ calculation is somewhat impaired despite the fair value $R^2 = 0.9614$, but values of constants $p1$ and $p2$ are in good compliance, e.g. with the data of Sellars [34] for C-Mn steel ($p1 = 0.5$, $p2 = 0.15$).

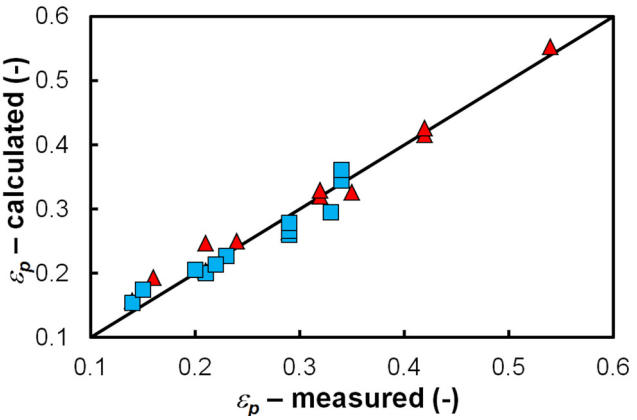

Fig. 9. Comparison of experimental and, according to Eq. (8), predicted values of $\varepsilon_p = f(D_0,Z)$ for low-alloy Mn-Ti-B steel (blue squares – direct heating to the deformation temperature; red triangles – preheating at 1200°C)

5. Conclusions

The examination was focused on the flow stress curves of low-alloy Mn-Ti-B steel, obtained by uniaxial compression tests at the temperatures of 900-1200°C and strain rates of 0.1-10 s^{-1}. One set of samples was heated directly to the deformation temperature, which corresponded to the initial austenitic grain size of 19-56 µm. The other set of samples was uniformly preheated at the temperature of 1200°C with the identical initial grain size of 56 µm.

The initial grain size D_0 affects the flow stress curves mainly at the low deformation temperatures when differences in the D_0 value of both sets of samples are significant. Whereas the values of peak stress σ_p and steady-state stress σ_{ss} practically do not depend on the parameter D_0 at all, the peak strain ε_p values of coarser-grained structure significantly increase mainly at high values of the parameter Z. This confirms the negative effect of the large size of the initial grain on the dynamic recrystallization kinetics, which can be explained by the reduction in nucleation density.

Equations were compiled for both sets of samples, describing both coordinates of the peak point as a function of the parameter Z (and in the case of peak strain, also including the effect of D_0) with fair accuracy. The calculated regressive constants associated with stress σ_p were affected by the initial grain size only to a minimum extent (see the activation energy value Q = 314.5 kJ·mol^{-1} when heating directly to the deformation temperature vs 316.5 kJ·mol^{-1} after preheating at high temperature).

From the methodological point of view, it is important that the parameters of austenization of samples of the examined steel before the compression tests (i.e. uniform preheating or, as the case may be, heating directly to the deformation temperature) significantly affect the dynamic recrystallization kinetics and values of $\varepsilon_p = f(Z)$, but almost do not affect stress $\sigma_p = f(T,\dot{\varepsilon})$. This is important for indicative prediction of maximum flow stress at the given temperature and strain rate. Not from a strictly scientific, but from a purely practical point of view, it appears to be more appropriate to heat the samples directly to the deformation temperature. In this case, the initial grain size better corresponds to the grain size gradually decreasing in operating multi-pass hot forming processes (e.g. rolling), when the microstructure of the gradually cooling semi-finished product is repeatedly refined mainly by post-dynamic recrystallization actions.

Acknowledgements

This paper was created at the Faculty of Metallurgy and Materials Engineering within the Project No. LO1203 "Regional Materials Science and Technology Centre – Feasibility Program" funded by the Ministry of Education, Youth and Sports of the Czech Republic; and within the students' grant project SP2018/105 supported at the VŠB – TU Ostrava by the Ministry of Education, Youth and Sports of the Czech Republic.

REFERENCES

[1] C. Rossard, Microstructure and Design of Alloys, in: The 3rd International Conference on the Strength of Metals and Alloys, Pergamon Press, Institute of Metals, London, (1973).

[2] A.I. Fernández, P. Uranga, B. López, J.M. Rodriguez-Ibabe, Mat. Sci. Eng. A. **361** (1-2), 367-376 (2003), DOI: 10.1016/S0921-5093(03)00562-8.

[3] C. Zener, J.H. Hollomon, J. Appl. Phys. **15** (1), 22-32 (1944).

[4] H.J. McQueen, J.J. Jonas, Treatise on Materials Science and Technology, R.J. Arsenault (Ed.), Academic Press, New York (1975).

[5] S.W. Xu, S. Kamado, T. Honma, Scripta Mater. **63** (3), 293-296 (2010), DOI: 10.1016/j.scriptamat.2010.04.012.

[6] A. Dehghan-Manshadi, P.D. Hodgson, Metall. Mater. Trans. A. **39A** (12), 2830-2840 (2008), DOI: 10.1007/s11661-008-9656-5.

[7] T. Sakai, J.J. Jonas, Acta Metall. **32** (2), 189-209 (1984), DOI: 10.1016/0001-6160(84)90049-X.

[8] J. Kliber, I. Schindler, W. Kubinski, Z. Kuzminski, Steel Res. **60** (11), 503-508 (1989), DOI: 10.1002/srin.198901693.

[9] P.J. Wray, Metall. Trans. A. **15** (11), 2009-2019 (1984), DOI: 10.1007/BF02646835.

[10] M.J. Luton, C.M. Sellars, Acta Metall. **17** (8), 1033-1043 (1969).

[11] H.Q. Liang, H.Z. Guo, K. Tan, Y.Q. Ning, X. Luo, G. Cao, J.J. Wang, P.L. Zhen, Mat. Sci. Eng. A. **638**, 357-362 (2015), DOI: 10.1016/j.msea.2015.04.046.

[12] A. Belyakov, H. Miura, T. Sakai, Mat. Sci. Eng. A. **255** (1-2), 139-147 (1998), DOI: 10.1016/S0921-5093(98)00784-9.

[13] D. Ohadi, M.H. Parsa, H. Mirzadeh, Mat. Sci. Eng. A. **565**, 90-95 (2013), DOI: 10.1016/j.msea.2012.12.030.

[14] Z.H. Wang, S.H. Sun, B. Wang, Z.P. Shi, R.H. Zhang, W.T. Fu, Metall. Mater. Trans. A. **45A** (8), 3631-3639 (2014), DOI: 10.1007/s11661-014-2290-5.

[15] D. Kuc, E. Hadasik, I. Schindler, P. Kawulok, R. Sliwa, Arch. Metall. Mater. **58** (1), 151-156 (2013), DOI: 10.2478/v10172-012-0166-5.

[16] A. Belyakov, H. Miura, T. Sakai, Scripta Mater. **43** (1), 21-26 (2000), DOI: 10.1016/S1359-6462(00)00373-0.

[17] M.R. Barnett, A.G. Beer, D. Atwell, A. Oudin, Scripta Mater. **51** (1), 19-24 (2004), DOI: 10.1016/j.scriptamat.2004.03.023.

[18] R. Ding, Z.X. Guo, Acta Mater. **49** (16), 3163-3175 (2001), DOI: 10.1016/S1359-6454(01)00233-6.

[19] M. El Wahabi, L. Gavard, F. Montheillet, J.M. Cabrera, J.M. Prado, Acta Mater. **53** (17), 4605-4612 (2005), DOI: 10.1016/j.actamat.2005.06.020.

[20] Y.B. Yang, Z.M. Zhang, X.B. Li, Q. Wang, Y.H. Zhang, Mater. Design. **51**, 592-597 (2013), DOI: 10.1016/j.matdes.2013.04.034.

[21] M.C. Sellars, W.J. McG. Tegart, Int. Metall. Rev. **17** (158), 1-24 (1972).

[22] I. Schindler, P. Kawulok, R. Kawulok, E. Hadasik, D. Kuc, High Temp. Mat. Pr. **32** (2), 149-155 (2013), DOI: 10.1515/htmp-2012-0106.

[24] H. Mirzadeh, M.H. Parsa, D. Ohadi, Mat. Sci. Eng. A. **569**, 54-60 (2013), DOI: 10.1016/j.msea.2013.01.050.

[25] M.C. Sellars, W.J. McG. Tegart, Mem. Etud. Sci. Rev. Metl. **63**, 731-746 (1966).

[26] S.F. Medina, C.A. Hernandez, Acta Mater. **44** (1), 137-148 (1996), DOI: 10.1016/1359-6454(95)00151-0.

[27] R. Colas, J. Mater. Process. Tech. **62** (1-3), 180-184 (1996), DOI: 10.1016/0924-0136(95)02227-9.

[28] Y.C. Lin, M.S. Chen, J. Zhang, Mat. Sci. Eng. A. **499** (1-2), 88-92 (2009), DOI: 10.1016/j.msea.2007.11.119.

[29] J. Cai, F.G. Li, T.Y. Liu, B. Chen, M. He, Mater. Design. **32** (3), 1144-1151 (2011), DOI: 10.1016/j.matdes.2010.11.004.

[30] L. Ou, Y.F. Nie, Z.Q. Zheng, J. Mater. Eng. Perform. **23** (1), 25-30 (2014), DOI: 10.1007/s11665-013-0747-0.

[31] S. Mandal, V. Rakesh, P.V. Sivaprasad, S. Venugopal, K.V. Kasiviswanathan, Mat. Sci. Eng. A. **500** (1-2), 114-121 (2009), DOI: 10.1016/j.msea.2008.09.019.

[32] H.Y. Wu, J.C. Yang, F.J. Zhu, C.T. Wu, Mat. Sci. Eng. A. **574**, 17-24 (2013), DOI: 10.1016/j.msea.2013.03.005.

[33] A. Mohamadizadeh, A. Zarei-Hanzaki, H.R. Abedi, Mech. Mater. **95**, 60-70 (2016), DOI: 10.1016/j.mechmat.2016.01.001.

[34] S.F. Medina, C.A. Hernandez, Acta Mater. **44** (1), 149-154 (1996), DOI: 10.1016/1359-6454(95)00152-2.

[35] C.M. Sellars, Hot working and forming processes, Metals Society, London, (1980).